Ion gyroresonance observations at Jicamarca revisited

F. S. Rodrigues,[1] M. J. Nicolls,[2] R. Woodman,[3] D. L. Hysell,[1] J. L. Chau,[4] and S. A. González[5]

Received 14 February 2007; revised 14 May 2007; accepted 6 June 2007; published 12 July 2007.

[1] This paper presents recent observations of the proton gyroresonance over Jicamarca. In October 2006, a single-polarization double-pulse experiment was set up to measure the first gyroresonance peak in the incoherent scatter (IS) auto-correlation function (ACF). Despite the clutter caused by Spread-*F* and artificial satellites, it was possible to measure the first proton gyroresonance peak of the ACF in the topside ionosphere. For the first time, least-squares fits of theoretical IS ACFs to gyroresonance measurements are reported. Theoretical ACFs that best fit the measurements were found using the H^+ fraction and temperature (assuming $T_e = T_i$) as fitting parameters. Uncertainties for the estimated fraction of H^+ were as low as 12%, while uncertainties for estimated temperatures were around 30%. These are the first successful gyroresonance measurements since the early observations of Farley (1967), and it is the first time measurements of this type have been used to obtain least squares estimates of ion composition and temperatures.

Citation: Rodrigues, F. S., M. J. Nicolls, R. Woodman, D. L. Hysell, J. L. Chau, and S. A. González (2007), Ion gyroresonance observations at Jicamarca revisited, *Geophys. Res. Lett.*, *34*, L13107, doi:10.1029/2007GL029680.

1. Introduction

[2] Radar observations of the topside ionosphere using conventional incoherent scatter (IS) methods are difficult. The low signal-to-noise ratio and the large number of artificial satellites are the main obstacles for topside IS radar observations. The first topside observations at the magnetic equator were made in the mid-1960's [*Farley*, 1966], but only recently have new radar techniques been designed for improved topside measurements at Jicamarca [*Hysell*, 2000]. This paper addresses the possibility of using a somewhat less conventional IS measurement for estimation of plasma parameters in the equatorial topside ionosphere. Inclusion of the magnetic field in IS theory leads to the prediction of a spectrum which oscillates with a period approximately equal to the ion gyroperiod superimposed on the otherwise smooth IS spectrum.

[3] This effect occurs at small aspect angles (i.e., when the radar beam is pointed close to perpendicular to the magnetic field) [e.g., *Farley et al.*, 1961; *Salpeter*, 1961]. The fluctuations in the IS spectrum map into peaks in the IS autocorrelation function (ACF) at lag times corresponding to multiples of the ion gyroperiod, $2\pi m_i/qB$ (where m_i is the ion mass, q is the ion charge, and B is the magnetic field intensity). For mixtures of ions, peaks should exist at the gyroperiods of each ion, suggesting a powerful ionospheric diagnostic for composition measurements.

[4] The physical explanation for the ion gyroresonance is quite intuitive. The ions move in helical orbits, with Larmor (gyro) motion superimposed on a guiding center drift. Near perpendicular incidence, a radar with a wavelength in the appropriate regime ($\lambda/4\pi$ greater than the Debye length but less than the ion gyroradius) will be sensitive to the periodic motion at the gyrofrequency in the absence of other forces that could decorrelate such a resonance [*Farley*, 1967].

[5] As reviewed by *Farley* [1967], the first attempts to measure the O^+ resonance were unsuccessful. It was then realized that ion-ion Coulomb collisions destroy the gyroresonance peak, the reason for the absence of the O^+ gyroresonance at *F*-region heights [e.g., *Farley*, 1964]. Thus, because the resonance is effectively destroyed, incoherent scatter calculations near perpendicular usually neglect the gyroresonance effect completely by not including the magnetic field in the calculation of the appropriate ion admittance function [e.g., see *Swartz and Farley*, 1979]. However, at higher altitudes where densities are lower and Coulomb collisions are less important, observations of the H^+ resonance are still possible.

[6] *Farley* [1967] made the first and the only published observations of the H^+ gyroresonance, showing that under the right conditions, one can measure the H^+ gyroresonance peaks. In his experiment, Farley was able to observe the first three H^+ gyroresonance peaks in the IS ACF. At the time Farley made his measurements, computation of theoretical ACFs was time consuming especially for small aspect angles, so that computer-based fits of the measured ACFs were virtually impossible. To illustrate the good agreement between his observations and the IS theory including the geomagnetic field, Farley plotted one example of his measured ACFs and a few theoretical ACFs provided by R. Woodman who was working on a full IS theory [*Woodman*, 1967] and had developed a technique to compute ACFs for small aspect angles [see also *Woodman*, 2004].

[7] In this work, observations of the proton gyroresonance at Jicamarca are revisited. The motivation for the renewed interest in the gyroresonance is the possibility of using these measurements to obtain estimates of the topside composition (fractions of O^+ and H^+) and topside temperatures, perhaps in combination with more standard measurements of the lower lags of the ACF. Another reason for new gyroresonance observations is that, the IS theory for small aspect angles has been improved recently so that the effect

[1]Cornell University, Earth and Atmospheric Sciences, Ithaca, New York, USA.
[2]SRI International, Center for Geospace Studies, Menlo Park, California, USA.
[3]Instituto Geofísico del Perú, Lima, Perú.
[4]Radio Observatorio de Jicamarca, Instituto Geofísico del Perú, Lima, Perú.
[5]Arecibo Observatory, Arecibo, Puerto Rico.

0094-8276/07/2007GL029680$05.00

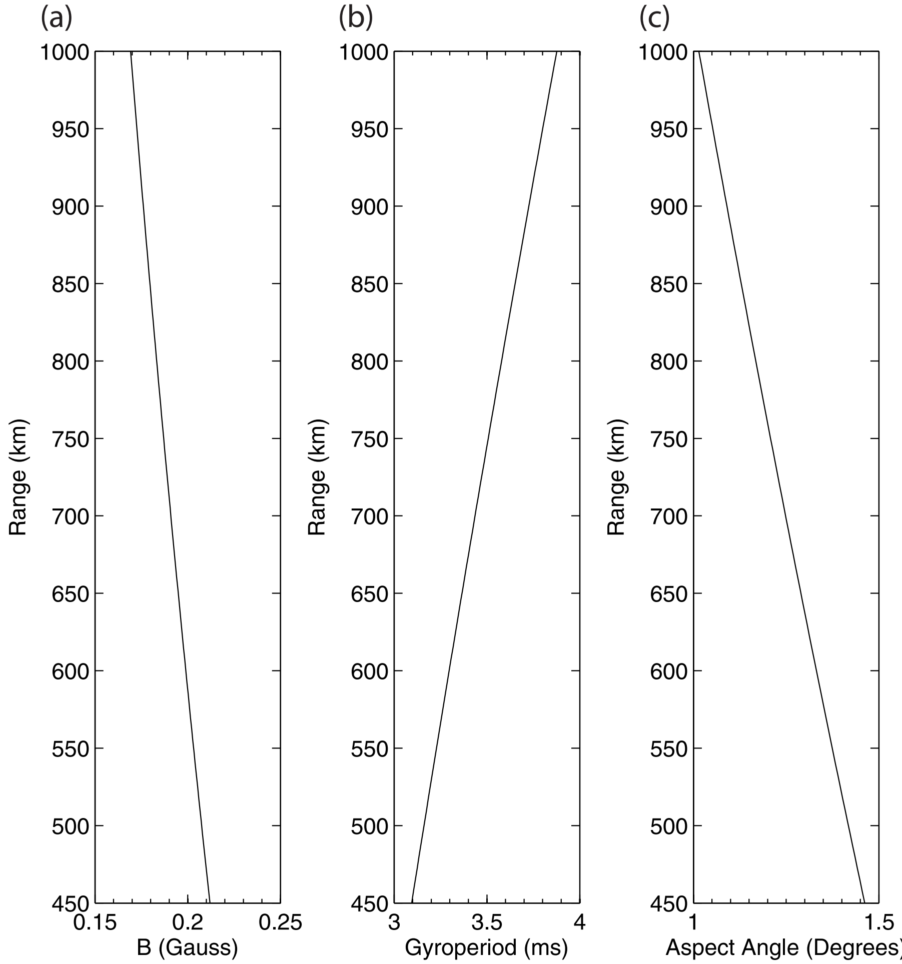

Figure 1. (a) Geomagnetic field intensity, (b) gyroperiod and (c) aspect angle as a function of range along the radar line-of-sight.

of electron Coulomb collisions in controlling the shape of IS spectrum is better understood [*Sulzer and González*, 1999; *Woodman*, 2004]. Below, the new experiment is described and examples of least-squares fits of theoretical ACFs to the observations are presented.

2. Experimental Setup

[8] For these observations, a single-polarization double-pulse setup was used. A single circular polarization was used so that two transmitters could be combined to improve the signal-to-noise ratio of the received echoes. Echoes with both circular polarizations were received and it was observed that depolarization effects were negligible. The two transmitters combined deliver a peak power of 2 MW. The on-axis configuration (declination $-12.88°$, hour angle $-4.617°$) of the Jicamarca antenna was also used in order to obtain the best antenna gain.

[9] The proton gyroperiod was calculated using values of the geomagnetic field from the International Geomagnetic Reference Field (IGRF) model for ranges along the line-of-sight of the radar. The gyroperiod varies between 3 and 4 milliseconds (ms) for topside (550–1000 km) ranges.

[10] Figure 1 shows the geomagnetic field values as a function of range along with the corresponding proton gyroresonance period and the angle the wave vector of the transmitted wave makes with the geomagnetic field for the on-axis antenna configuration. The aspect angle becomes very small (varying from 1.5 to 1.0 degrees) in the 550–1000 km range, and electron Coulomb collisions can become an important factor in determining the shape of the IS spectrum.

[11] Five equally spaced lags between 3.1 and 3.9 ms were measured using double pulses. The zero lag (power) was measured with a single pulse before each transmission of the set of five double pulses. The single pulse provides normalization for the measured ACF, and combined with digisonde measurements of f_0F2, gives electron density estimates for the F region and topside. The pulses used in this experiment were 0.5 ms (75 km) long, and the inter-pulse period was 2500 km. The sampling frequency was 20 kHz, giving range gates every 7.5 km.

[12] The experiment was conducted on the evenings of October 10 and 11, 2006. A major difficulty of an experiment of this type is clutter (i.e., unwanted signals) from the F region, coherent echoes from Spread-F, and satellites/space debris. The former contaminant is pulse-to-pulse clutter

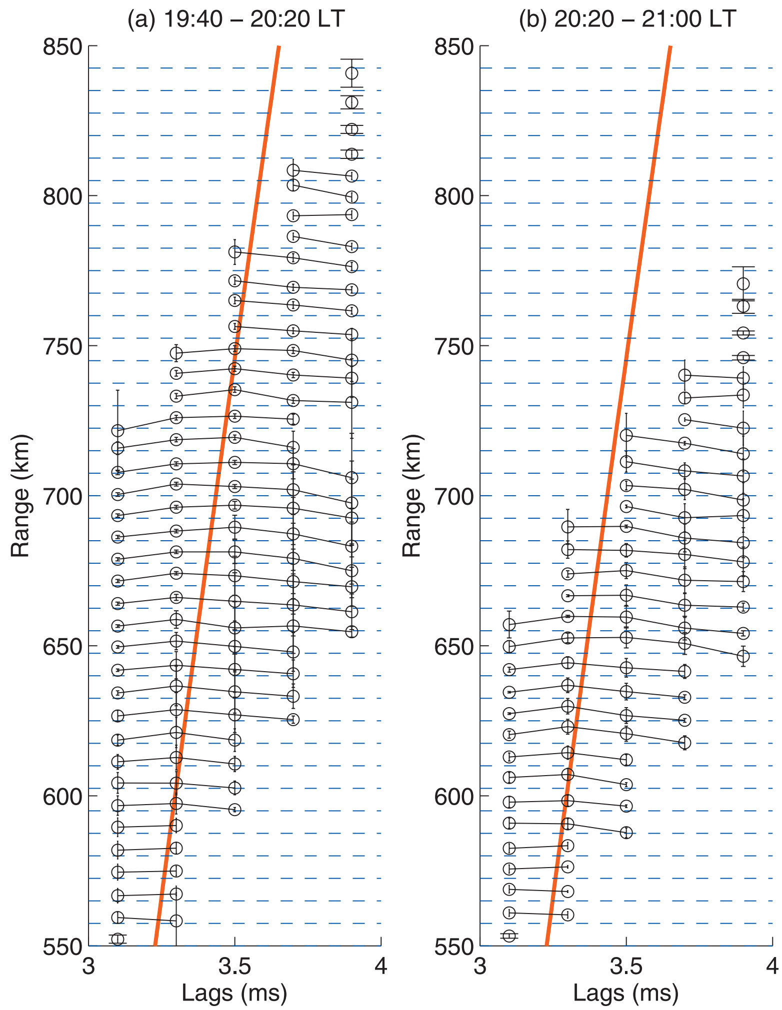

Figure 2. (a) Incoherent scatter autocorrelation functions measured on 1940–2020 LT October 10, 2006. The solid diagonal line shows the values of the gyroperiod based on IGRF. Vertical spacing between dashed lines correspond to a correlation of 0.5. (b) Same except for 2020–2100 LT.

resulting from the long spacings required to measure the appropriate lags. This clutter is removable to some degree. Unfortunately, on both nights Spread-*F* events were observed. They started with a bottom-type layer around 19 LT and developed into coherent scatter radar plumes reaching the topside ionosphere. Spread-*F* coherent echoes contaminated IS echoes after 21 LT, making gyroresonance observations impossible. However, it was possible to use data from the early evening hours after eliminating data affected by satellites and space debris.

[13] The estimator for the normalized ACF (ρ) is given by:

$$\hat{\rho} = \frac{\langle V_t V_{t+\tau}^* \rangle}{S} \qquad (1)$$

where $\langle \ldots \rangle$ represents the expected value of its argument, V_t and $V_{t+\tau}$ are complex voltage samples spaced by the time delay τ, and S is the signal power. S is estimated from the single-pulse transmissions. When noise and clutter are taken into consideration, it can be shown that the variance for the normalized ACF is given by:

$$\langle |\hat{\rho} - \langle \hat{\rho} \rangle|^2 \rangle = \frac{1}{K} \left(\frac{S+N+C}{S} \right) \left(1 + |\rho|^2 \right) \qquad (2)$$

where K is the number of measurements used to estimate the normalized ACF (ρ). S, N and C are the signal, noise and clutter power, respectively. While S and N are obtained from the power profile of the single-pulse transmissions, estimates of C for each measured lag are obtained from the power profile of the double-pulse transmissions.

3. Results and Discussion

[14] Figure 2 shows two consecutive profiles of gyroresonance measurements during the evening of October 10. The plots show measured ACFs as a function of range together with measurement errors. Horizontal dashed lines indicate the zero correlation level for each ACF, and the

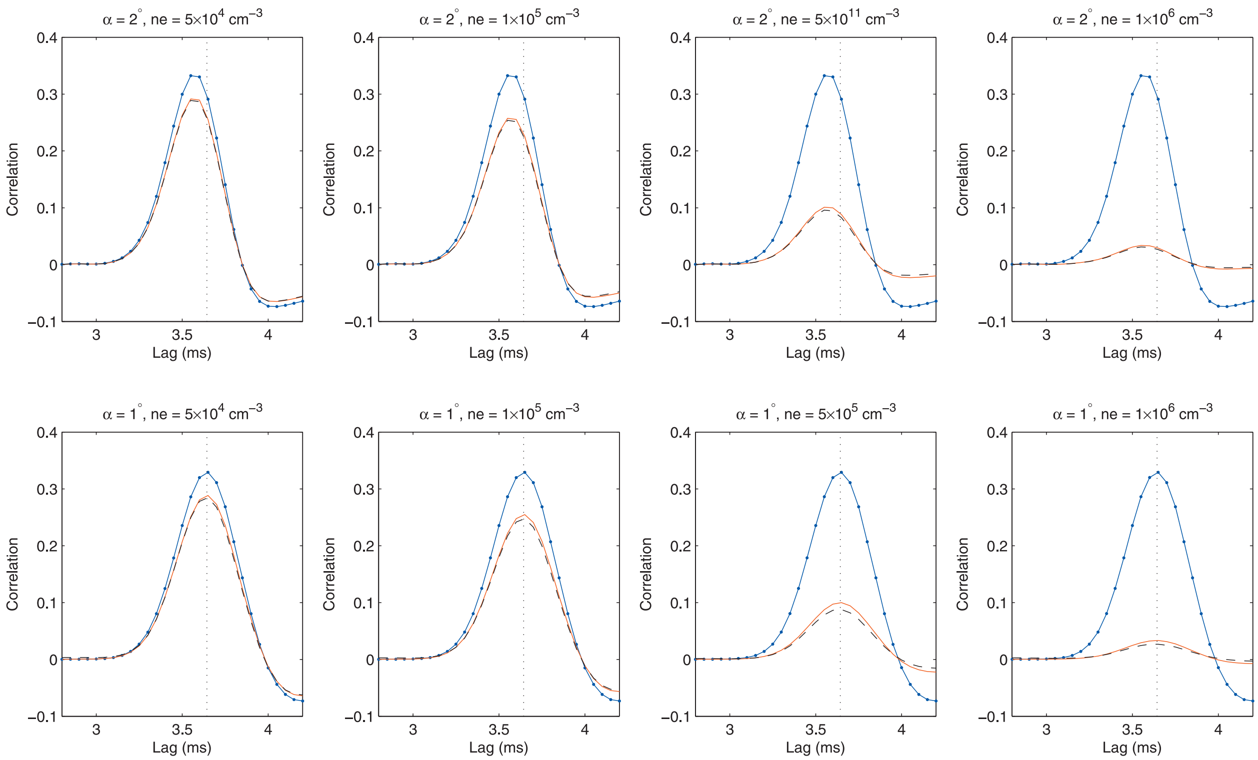

Figure 3. Theoretical curves for the gyroresonance. All curves correspond to $B = 18000$ nT, $T_e = T_i = 1000$ K and $H^+ = O^+ =$ 50%. Electron density and aspect angles are indicated in each plot. The dotted lines correspond to no collisions, the solid lines correspond to ion Coulomb collisions, and the dashed lines correspond to both ion and electron Coulomb collisions. The vertical dotted line in each plot indicates the proton gyroresonance period.

vertical spacing between dashed lines correspond to a correlation of 0.5. Each plot is the result of a 40-minute incoherent integration. ACF values affected by clutter were identified and removed. The diagonal solid line shows the gyroperiod as a function of range.

[15] The peak in the ACF is very close to the gyroperiod in almost every range gate. The maximum correlation increases with altitude, indicating an increase in the H^+ fraction with height, as expected. The gyroresonace peak was not detected below 550 km and above 850 km. It is likely that there was no detectable amount of H^+ below about 550–575 km and that the sensitivity was too low for detection above 850 km.

[16] In order to estimate temperatures and composition from our gyroresonance measurements, theoretical IS ACFs that best match the measurements were found using a least-squares algorithm. When computing theoretical ACFs, it is important to include ion-ion Coulomb collisions, as they play an important role in reducing the magnitude of the correlation through probabilistic diffusion [*Farley*, 1964; *Woodman*, 1967]. The gyro-peak is affected by the H^+ fraction as well as the electron density because of the effects of collisions; since the electron density decreases with increasing altitude on the topside, so does the ion-ion Coulomb collision frequency, which means that for a given H^+ fraction the peak of the resonance will be larger. The width of the gyro-peak is largely determined by the temperature. In the analysis, it was found that the shape of the gyro resonances is weakly affected by the amount of electron Coulomb collisions. Nevertheless, electron Coulomb collisions were incorporated in the theoretical model.

[17] The main effects of electron Coulomb collisions on the shape of the IS spectrum (or ACF) and its dependence on the aspect angle were explained by *Sulzer and González* [1999]. IS ACFs for a collisional magnetized plasma were calculated using the formulation described by *Woodman* [1967] and *Kudeki and Milla* [2006]. For the electron Gordeyev integral, we used the numerical library provided by *Sulzer and González* [1999].

[18] Some examples are shown in Figure 3, where theoretical curves show the dependence of the gyroresonance with electron density. At low densities, collision frequencies are low and thus both ion and electron Coulomb collisions have a small effect on the shape of the gyro hump. As the density increases, the ion Coulomb collision frequency increases and destroys the resonance completely. At intermediate densities, electron Coulomb collisions provide a small correction to the shape of the gyroresonance. Closer to perpendicular, the role of collisions becomes more important, the gyro-peak moves to greater lags and is broadened somewhat. This is because at small angles (less than the so-called critical angle, $\sqrt{m_e/m_i} \approx 1.34°$ for hydrogen) the dynamics of the electrons become more important, and the simple intuitive explanation for the gyroresonance mentioned in the introduction is no longer valid. In effect, that explanation assumed that the electrons could shield the ions by moving along the field lines. Close to perpendicular, the effective mass of the electron gets

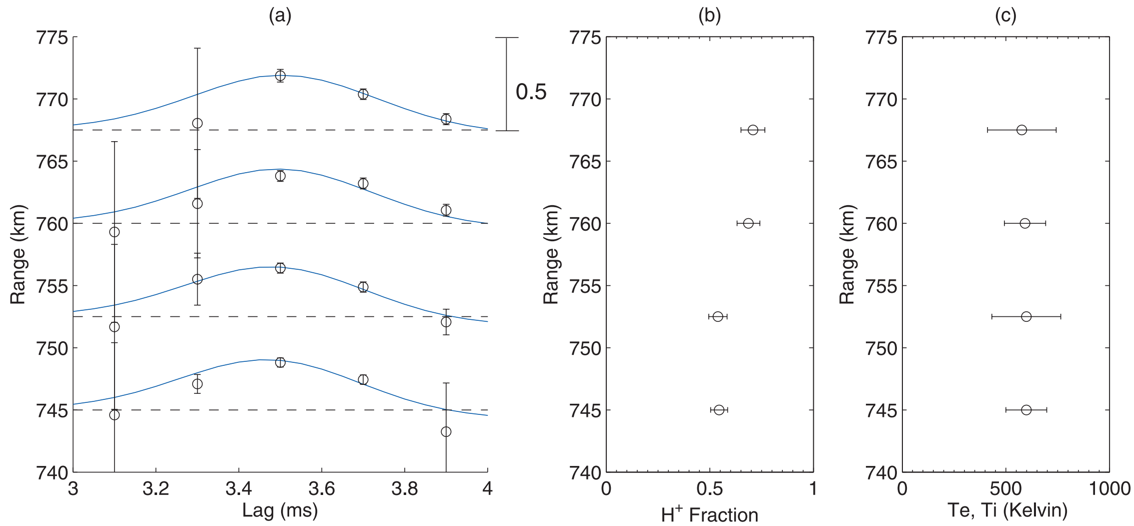

Figure 4. (a) Examples of theoretical ACFs that best match a set of measured gyroresonance measurements for October 10 2006, 1900–2000 LT (see scale on the top right side of the plot). Also shown are (b) inverted H^+ fractions and (c) temperatures.

scaled by a factor 1/sin α, where α is the angle off perpendicular, so that the electrons appear to have more inertia and cannot shield out the ions as effectively. This role causes the gyroresonance to move to higher lags as the electrons diffuse away more slowly [e.g., *Woodman*, 1967].

[19] An error-weighted general least-squares method was used to find theoretical curves that best fit the measurements. Fits were constrained to the isothermal case ($T_e = T_i$), which is a reasonable assumption at night. Topside electron density estimates were obtained from the height profiles of the signal power measured by the radar and calibrated by the F-peak electron density (f_0F2) measured by the Jicamarca digisonde. Figure 4 shows examples of ACFs measured at consecutive range gates, and the respective best fits to the data. The best fit ACFs match the data within the error bars. The fits in Figure 4 are shown for data integrated for one hour. Longer integration time was used to improve the statistics. Other ACFs have two or more lags affected by clutter, and the resulting fits are not conclusive due to large errors in the estimated parameters.

4. Conclusion

[20] Proton gyroresonance was observed over Jicamarca using a new experiment setup. Observations were limited to periods without Spread-*F*, which contaminates the data with strong coherent echoes. Despite the clutter from *F*-region IS echoes, it was possible to find theoretical curves that best fit our measurements giving reasonable values of temperature and H^+ fraction. The theoretical predictions from IS theory are in good agreement with the observations. The fitting procedure takes into account both ion and electron Coulomb collisions, both of which affect the IS ACFs at small aspect angles. Temperatures were estimated with a 30% uncertainty, while H^+ concentration estimates had errors as small as 12%. For periods with reduced clutter from coherent echoes, the gyroresonance can be measured with higher accuracy, and the uncertainties in the estimated parameters will be reduced. The gyroresonance was not detected in the early morning hours when the electron density and signal-to-noise ratio become very low. While the best observations were made on the evening of October 10, gyroresonance was also observed on October 11.

[21] As a result of the clutter from *F*-region coherent and IS echoes, only a few complete five-lag ACFs were observed. More accurate measurements and more precise estimates of H^+ and temperatures are possible during periods when coherent echoes are not present. During those periods, measurements of the gyroresonance may be useful for H^+ detection and temperature estimation. This would be important for studies of temperatures in the topside ionosphere and light ions dynamics in the equatorial region. The possibility of estimating parameter profiles from gyroresonance observations during nights without Spread-*F* events, and using more sophisticated inversion techniques is being investigated.

[22] **Acknowledgments.** FSR is thankful for valuable discussions with D. Farley. The Jicamarca Radio Observatory is a facility of the Instituto Geofísico del Perú and is operated with support from the NSF Cooperative Agreement ATM-0432565 through Cornell University. FSR and MJN performed the experiments with partial support from Jicamarca's visiting program.

References

Farley, D. T. (1964), The effect of coulomb collisions on incoherent scattering of radio waves by a plasma, *J. Geophys. Res.*, *69*, 197–200.
Farley, D. T. (1966), Ionospheric temperatures and composition measurements at the magnetic equator, *Ann. Geophys.*, *22*, 448–453.
Farley, D. T. (1967), Proton gyroresonance observed in incoherent scattering from the ionosphere, *Phys. Fluids*, *10*(7), 1584–1586.
Farley, D. T., J. P. Dougherty, and D. W. Barron (1961), A theory of incoherent scattering of radio waves by a plasma II. Scattering in a magnetic field, *Proc. R. Soc. London, Ser. A*, *263*, 238–258.
Hysell, D. L. (2000), Incoherent scatter experiments at Jicamarca using alternating codes, *Radio Sci.*, *35*(6), 1425–1436, doi:10.1029/2000RS002368.

Kudeki, E., and M. Milla (2006), Incoherent scatter spectrum theory for modes propagating perpendicular to the geomagnetic field, *J. Geophys. Res.*, A06306, doi:10.1029/2005JA011546.

Salpeter, E. E. (1961), Plasma density fluctuations in a magnetic field, *Phys. Rev.*, *122*, 1663–1674.

Sulzer, M. P., and S. A. González (1999), The effect of electron Coulomb collisions on the incoherent scatter spectrum in the *F* region at Jicamarca, *J. Geophys. Res.*, *104*, (A10), 22,535–22,551.

Swartz, W. E., and D. T. Farley (1979), A theory of incoherent scattering of radio waves by a plasma: 5. The use of the Nyquist theorem in quasi-equilibrium situations, *J. Geophys. Res.*, *84*, (A5), 1930–1932.

Woodman, R. F. (1967), Incoherent scattering of electromagnetic waves by a plasma, Ph.D. thesis, Harvard University, Cambridge, Massachusetts.

Woodman, R. F. (2004), On a proper electron collision frequency for a Fokker-Planck collision model with Jicamarca applications, *J. Atmos. Solar-Terr. Phys.*, *66*(17), 1521–1541.

J. L. Chau, Radio Observatorio de Jicamarca, Instituto Geofísico del Perú, Apartado 13-0207, Lima 13, Peru.

S. A. González, Arecibo Observatory, HC3 Box 53995, Arecibo, Puerto Rico 00613-0995.

D. L. Hysell and F. S. Rodrigues, Cornell University, 2122 Snee Hall, Ithaca, NY 13205, USA. (fsr5@cornell.edu)

M. J. Nicolls, SRI International, 333 Ravenswood Ave., Menlo Park, CA 94025-3493, USA.

R. Woodman, Instituto Geofísico del Perú, Apartado 13-0207, Lima 13, Peru.